

# Stacking and Analyzing $z \approx 2$ MOSDEF Galaxies by Spectral Types: Implications for Dust Geometry and Galaxy Evolution

BRIAN LORENZ <sup>1</sup>, MARISKA KRIEK <sup>2</sup>, ALICE E. SHAPLEY <sup>3</sup>, RYAN L. SANDERS <sup>4</sup>, ALISON L. COIL <sup>5</sup>, JOEL LEJA <sup>6</sup>, BAHRAM MOBASHER <sup>7</sup>, ERICA NELSON <sup>8</sup>, SEDONA H. PRICE <sup>9</sup>, NAVEEN A. REDDY <sup>7</sup>, JORDAN N. RUNCO <sup>3</sup>, KATHERINE A. SUESS <sup>10</sup>, IRENE SHIVAEI <sup>11</sup>, BRIAN SIANA <sup>7</sup>, AND DANIEL R. WEISZ <sup>1</sup>

## 1. Introduction

- crucial measurements (metallicity, dust-corrected SFR) require detections of the faint H $\beta$  line
- H $\beta$  grows fainter in dusty galaxies which tend to be more massive
- large samples can be leveraged by **stacking spectra** and **photometry** to increase the signal
- risk of stacking: combining galaxies with different properties & washing out spectral features
- use photometry to **group galaxies with similar spectral types**
- study of dust and metal with different galaxy types

## 2. Data

- 660 galaxies** from MOSFIRE Deep Evolution Field (MOSDEF) Survey
- ~1500 H-band selected galaxies in CANDLES fields using MOSFIRE spectrograph
- need coverage of H $\alpha$  and H $\beta$  lines
- $1.37 \leq z \leq 1.70$ ,  $2.09 \leq z \leq 2.61$  (H $\alpha$  falls in a band of atmospheric transmission)
- 408:  $3\sigma$  detected H $\alpha$  and H $\beta$ , 196: only  $3\sigma$  detected H $\alpha$ , 56: neither line detected at  $3\sigma$

## 3. Data Analysis

- group galaxies by SED shape, using spectroscopic redshifts and observed fluxes
- form composite SEDs in each group
- stack spectra: median-stacked in the rest-frame
- fit 6 emission lines (H $\beta$   $\lambda$ 4863, [OIII]  $\lambda$ 4960 and  $\lambda$ 5008, H $\alpha$   $\lambda$ 6565, [NII]  $\lambda$ 6550 and  $\lambda$ 6585) in each stacked spectra

- H $\alpha$ /H $\beta$ , [NII]  $\lambda$ 6585/H $\alpha$ , [OIII]  $\lambda$ 5008/H $\beta$ , O3N2
- calculate dust-corrected H $\alpha$  SFRs for each composite SED groups
- $A_{V,neb} = R'_V \times 2.32 \times \log_{10} \left( \frac{H\alpha/H\beta}{2.86} \right)$  ( $R'_V = 3.1$ )  $\rightarrow$  compute the dust corrected H $\alpha$  luminosity
- $SFR = L(H\alpha) \times 10^{-4} \frac{M_{\odot} yr^{-1}}{erg s^{-1}}$   $\rightarrow$  dust-corrected SFRs
- measure metallicity
- $O3N2 = \log_{10} \left( \frac{[OIII]\lambda 5008/H\beta}{[NII]\lambda 6585/H\alpha} \right)$ ,  $12 + \log_{10}(O/H) = 8.97 - 0.39 \times O3N2$
- measure SED-based SFRs and dust properties
- fit the SED fitting code Prospector  $\rightarrow$  composite SED  $\rightarrow$  SED-based SFRs
- reasonable agreement with H $\alpha$  SFRs (Figure 3)

## 4. Results

- UVJ diagram (top-left of Figure 4)
  - more massive galaxies towards top-right of the star-formation sequence
  - most massive group is offset from the sequence, towards bluer V-J
- H $\alpha$  sSFRs vs mass (top-right of Figure 4)
  - H $\alpha$  sSFRs are in good agreement with SFMS (Leja et al 2021)
- BPT diagram
  - strong agreement with individual measurements of MOSDEF galaxies (Shapley et al 2015)
- mass-metallicity (bottom-right of Figure 4)
  - tight relation with higher mass galaxies showing higher metallicities
  - results (mean  $z=1.9$ ) are consistent with previous MOSDEF mass-metallicity relations
- dust properties: compare stellar  $A_V$  (measured from the composite SED) and nebular  $A_V$  (measured from Balmer decrements)
  - Figure 6
    - stellar  $A_V$ : moderate relation with SFR, strong relation with mass and metallicity
    - nebular  $A_V$ : strong relation with mass and SFR, moderate relation with metallicity
  - Figure 7
    - nebular  $A_V$  is larger than stellar  $A_V$  by roughly a factor of 2
    - strong trend between  $A_V$  excess and SFR

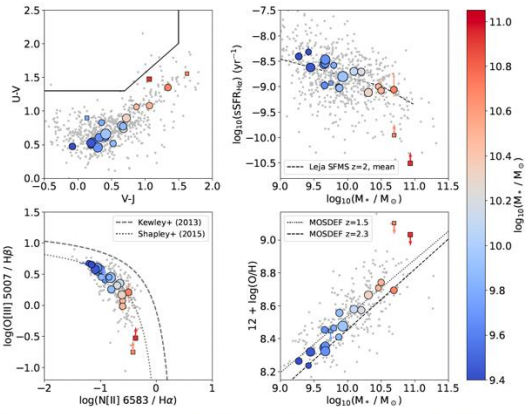


Figure 4: Overview of basic properties of the galaxy groups (color, with the same size and symbols as Figure 3)

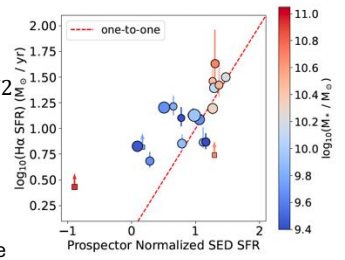


Figure 3: Prospector SFR derived from composite SEDs vs. Balmer decrement-corrected H $\alpha$  SFR from the stacked spectra. Point size scales with the number

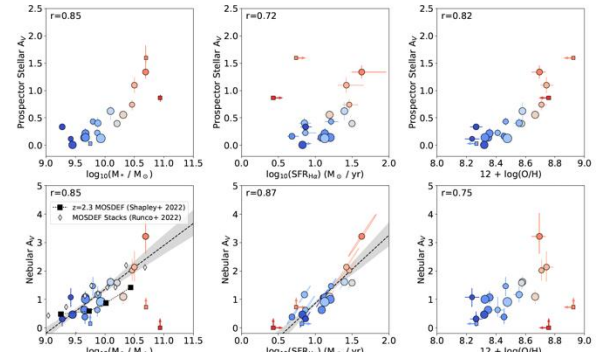


Figure 6: Top row: Stellar  $A_V$  (derived from Prospector composite SED fits) vs mass (left), SFR (center), and metallicity (right) for the 20 galaxy groups. Bottom row: Nebular  $A_V$  (derived from stacked spectra Balmer decrement) vs mass (left), SFR (center), and metallicity (right). Symbols and colors are the same as in Figure 3. Correlation coefficients are listed in the top-left of each panel. For the nebular  $A_V$  vs. mass and SFR (lower-left and lower-middle),

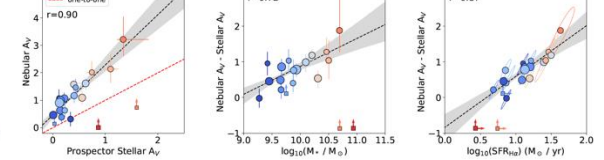


Figure 7: Symbols and colors are the same as in Figure 3. Left: Nebular  $A_V$  vs. stellar  $A_V$ . The properties are well-correlated, with nebular  $A_V$  being larger than stellar  $A_V$  by roughly a factor of 2 for all groups with H $\beta$  detections. Middle: Nebular  $A_V$  - stellar  $A_V$  ( $A_V$  excess) vs. mass. Right:  $A_V$  excess vs. SFR. Uncertainties are shown as

## 5. Discussion

- most massive group
  - offset from star forming sequence in the UVJ diagram  $\Rightarrow$  evolutionary path along the UVJ diagram
  - galaxies grow in stellar mass and their sSFRs drops
  - $\rightarrow$  drop down the star forming sequence before moving to the quiescent side
- decrease in sSFR, stellar  $A_V$  and nebular  $A_V$ 
  - $\Rightarrow$  high-mass galaxies shut down star formation and expel or destroy ISM dust
- H $\alpha$  SFR is higher than SED-based SFR
  - $\Rightarrow$  some H $\alpha$  emission may originate from AGN or hot evolved stars
- both stellar and nebular attenuation strongly correlate with galaxy mass
  - more massive galaxies form more stars over their lifetime and have larger gravitational potentials
  - $\rightarrow$  release more metals and dust into ISM
  - $\rightarrow$  higher metallicity gas leads to a higher dust-to-gas ratio
  - $\rightarrow$  higher dust column density in new star-forming regions where the bulk of the attenuation takes place
- excess of nebular  $A_V$  correlates with SFR
  - at high SFR, a significant fraction of the star formation would occur in highly-obscured regions
  - $\rightarrow$  produce strong nebular attenuation and little contribution to the stellar  $A_V$
  - $\rightarrow$  excess nebular attenuation
- at low SFR, there would not be highly-obscured star-formation
  - $\rightarrow$  nebular  $A_V$  and stellar  $A_V$  are produced from the same regions
  - $\rightarrow$  excess towards 0
- the highly-obscured star-formation region may take place in the star-forming clumps or galaxy centers

## 6. Conclusion

- composite SEDs and stacked spectra enable measurements that are not possible for all individual galaxies
- SED-based SFRs seems predict H $\alpha$  SFRs
- composite SEDs represent multiple evolutionary stages of galaxies
- stellar  $A_V$  correlate with stellar mass and metallicity, nebular  $A_V$  correlate with stellar mass and SFR
- excess  $A_V$  correlate with SFR
- By JWST, precise measurements of emission line in individual galaxies, access for Paschen lines, and precise observations of the location of the galaxies